JOURNAL OF MATERIALS SCIENCE 20 (1985) 2265–2274

Ultrasonic examination of reaction bonded silicon nitride

J. S. THORP, T. G. BUSHELL
Department of Applied Physics and Electronics, University of Durham, Durham, UK

An ultrasonic examination has been made of a series of partially nitrided reaction-bonded silicon nitride (RBSN) ceramics whose weight gains varied from 22% to nearly 64% representing full nitridation. A pulse echo overlap technique was used which enabled both the longitudinal and shear velocities of propagation to be measured at 15 MHz; from these measurements values of Young's modulus (E) and the bulk modulus (K) at room temperature were derived. For fully nitrided RBSN the values obtained were $E = 160$ GN m^{-2}, $K = 90$ GN m^{-2} in good agreement with published values obtained by ultrasonic methods. Both Young's modulus and the bulk modulus were found to be markedly sensitive to the changes in fractional porosity due to changes in weight gain (and green density) each decreasing by over 50% as the fractional porosity increased from 0.16 for a fully nitrided ceramic to 0.26 for 60% weight gain material.

1. Introduction

Silicon nitride has for some years been established as a leading refractory ceramic [1, 2]. It combines a range of properties not found in many other high temperature ceramics, namely high temperature compressive and impact strength, good surface hardness and abrasion resistance, a low coefficient of thermal expansion, good thermal shock resistance and chemical stability. These properties have led to engineering applications in hostile environments, some examples being firstly in gas turbines a replacement for metal alloys in key areas such as blade assemblies, heat exchangers and combustion chambers and secondly in the smelting industry where it is found that silicon nitride is virtually unaffected by molten metals, such as zinc and aluminium, which rapidly degrade conventional stainless steel containers. The dielectric properties of silicon nitride have also been of interest for many years because of the potential applications in electronics and device passivation. The properties of thin film Si_3N_4 were first summarized some years ago by Milek [3] and more recently interest has arisen in the dielectric properties of bulk material, particularly for microwave windows and radomes where the excellent thermal shock resistance is advantageous. This area of interest illustrates a general point also applicable in other applications, namely that the physical parameters of Si_3N_4 are very dependent on the detailed method of preparation; thus, for example, although the first microwave permittivity data for reaction bonded silicon nitride (RBSN) was given by Wells [4] in 1964, it was not until eight years later that Walton [5] reported the manufacture of low loss material by slip-casting silicon.

There are two widely-used methods of manufacturing silicon nitride, hot pressing and reaction bonding. In the former the product (HPSN) can have a density close to theoretical, is virtually pore-free and predominately shows the α-Si_3N_4 structure [2, 6]; in the latter a material (RBSN) is formed which typically has only about 80% theoretical density and may contain amounts of unreacted silicon dependent on the care taken in processing. The method of manufacture of RBSN leads to an ability to form complex shapes which is absent with HPSN. This arises because the green ceramic first formed from silicon powder by pressure sintering, injection moulding or slip casting is relatively soft and is easily machined; on nitriding dimensional stability of about 0.1% can be maintained so that only a light dressing off operation is required in contrast to the formidable

0022–2461/85 $03.00 + .12

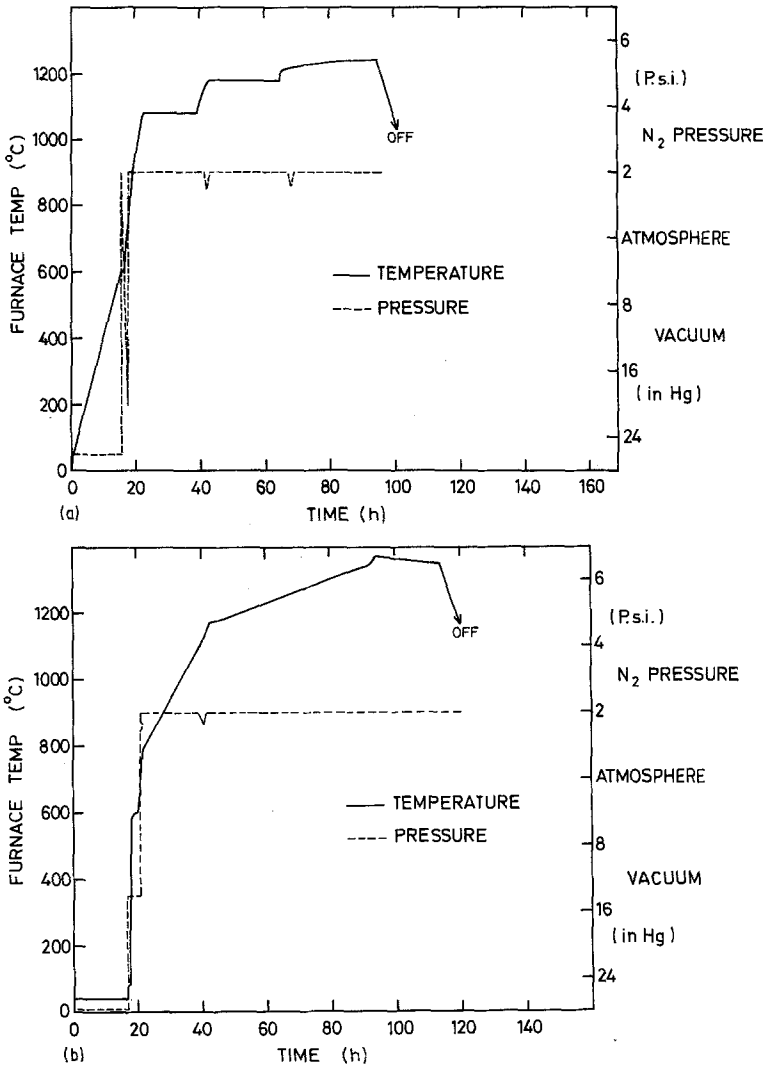

Figure 1 (a) Furnace schedule monitored for run 2, 32–35% weight gain. (b) Furnace schedule monitored for run 5, 44–49% weight gain.

post-manufacturing machining required for HPSN. Thus RBSN possesses some clear advantages in engineering applications providing that its other physical parameters are satisfactory for the purpose envisaged and it is likely that sintered silicon nitride will replace hot-pressed silicon nitride for most applications requiring dense material.

In the present work a series of specially prepared RBSN samples representing different degrees of nitridation have been examined in an attempt to clarify the role of free silicon in determining some of the physical properties; in this paper attention is directed to the elastic properties while corrresponding studies of the conductivity and dielectric behaviour will be presented separately.

2. Characterization of RBSN specimens

The specimens examined here were made, (at Advanced Engineering Materials Ltd, Gateshead currently located at Ruabon, Clwyd), using a modification of the standard commercial method. The starting material was micronized silicon powder whose major impurities were iron, aluminium and calcium (in amounts of 0.45, 0.25 and 0.05 weight per cent respectively) and in which 90% of particles had sizes less than 30 μm. The green ceramics were produced by sintering billets isostatically pressed at 185 MN m^{-2} and temperatures of 1200° C in an argon atmosphere. They were nitrided in an electrically heated furnace employing silicon carbide electrodes which was operated under a slight positive pressure of dry nitrogen such that the nitrogen was supplied according to reaction demand. Examples of the furnace temperature and pressure profiles designed to produce incomplete nitridation are shown in Fig. 1; in

TABLE I: Preparation and composition data for the silicon nitride ceramics examined

Firing run	Range of weight gain (%)	Nitrided density ($kg\ m^{-3}$)	C_p	C_{si}	C_{sn}	Density "green" ceramic ($kg\ m^{-3}$)	Peak temperature (° C)
1	18–22	1.95	0.281	0.391	0.327	1.60	1250
2	32–35	2.15	0.252	0.264	0.484	1.60	1240
3	34–42	2.24	0.238	0.206	0.555	1.60	1150
4	39–44	2.25	0.235	0.190	0.575	1.60	1340
5	44–49	2.35	0.221	0.132	0.646	1.60	1370
6	52–58	2.40	0.214	0.100	0.646	1.60	1440
7	55–59	2.54	0.195	0.015	0.790	1.60	1440
8	62–65	2.52	0.196	0.021	0.783	1.53	1440

making the range of partially nitrided ceramics the degree of nitridation was controlled by alteration of the furnace profile. At the levels of iron present, iron promoted growth of silicon nitride [1, 2] occurred giving an α:β phase ratio of about 1.5. The degree of nitridation referred to previously is conventionally called the "weight gain" of the ceramic. This figure is an expression of the percentage by which the weight of the green ceramic has increased in the reaction. The maximum possible weight gain is 66.5%, which is calculated by assuming that all the available silicon is converted to silicon nitride. In practice the maximum weight gain which is achieved is about 64.5%, which implies that a small amount of free silicon remains in the reacted nitride and that the reaction is limited not by silicon exhaustion, but by the inability of nitrogen to reach the remaining silicon.

The phase composition of RBSN ceramics has a marked effect on their properties and may be calculated [1] using the relationships

$$C_p = 1 - 0.281\,\rho_g - 0.148\,\rho_n \quad (1)$$

$$C_{si} = 1.072\,\rho_g - 0.643\,\rho_n \quad (2)$$

$$C_{sn} = 0.791\,(\rho_n - \rho_g) \quad (3)$$

where C_p, C_{si} and C_{sn} are, respectively the volume fractions of porosity, Si, and Si_3N_4 in a nitrided compact. ρ_g is the density of the green ceramic, and ρ_n the density of the nitrided material. The value of C_p, C_{si} and C_{sn} calculated for the materials used in this work are given in Table I. Further details of the preparation of the ceramics have been given by Bushell [7].

3. Experimental details

3.1. Specimen and bond fabrication

Preliminary pulse-echo measurements showed that in order to obtain good echo-trains, specimens having thicknesses of about a centimetre were required. Fortunately it was possible to obtain bulk pieces of material of each of the various degrees of nitridation which were sufficiently large for specimens to be cut from them with dimensions rather over 1 cm cube. This cutting, although rather a slow operation, was successfully completed using a diamond wheel saw. The subsequent specimen preparation is very important to the success of ultrasonic experiments because, to support an echo-train, it is vital that the reflecting faces be parallel; if they are not, the path of the waves moves away from the original propagation direction after repeated reflections and this causes gross distortion of the echo-train as a result of the transducer receiving different phases of wave across its diameter. Each specimen had opposite cube faces carefully polished flat and parallel using a Logitech precision lapping machine with successively finer grades of diamond paste (down to 1 μm). The surface finish of the faces is very important since a good bond can only be made to a smooth flat surface. At 15 MHz, the operating frequency used here, degrees of parallelism and flatness of 1 part in 10^4 (and a surface smoothness achieved using a 1 μm diamond paste) were required. Precision micrometer dial gauges and interferometric methods were used to check the flatness and parallelism of the faces.

Quartz piezoelectric transducers were used to generate and detect ultrasound in the specimens of reaction bonded silicon nitride. Crystal plate transducers were chosen because they could be moved to different places on a sample face and the polarization direction could be rotated if required. Standard "X-cut" and "Y-cut" 15 MHz transducers were used (supplied by Brooke's Crystal Co Ltd). These transducers were cut as discs with faces normal to the X and Y axes respectively so that an

alternating electric field parallel to the axis produced vibration in the direction parallel to the X-axis in the first case (longitudinal transducer) and normal to the Y-axis in the second case (shear transducer). The shear transducers used were marked with a flat parallel to the vibration direction. The resonant frequency of a transducer is determined by its thickness and the appropriate velocity of sound in the quartz; for megahertz operation, transducers need to be thin and are therefore fragile. Two sizes of transducer (1 cm or 6 mm in diameter) were used and gold plating allowed contact to be made to both electrodes from one side giving an active area approximately equal to that of the centre electrode.

Crystal plate transducers must be attached to the specimens under test by use of a suitable bonding agent. The bond formed must be thin and parallel and provide good acoustic coupling for both longitudinal and shear waves. Many different solid or liquid bonding agents are in general use but here the most suitable bonding materials have been found to be Dow resin 276-V9, Nonaq stopcock grease and phenyl salicylate (8–10). In making measurements on single crystals it may be important that transducers, especially those producing shear waves, are carefully aligned with the crystal axes. In this case a bonding material such as the Dow resin is particularly suitable, allowing as it does, transducer movement. In the present work, the polycrystalline nature of the RBSN samples meant that this freedom was not required, so phenyl salicylate bonds were used predominantly. In order to form a bond the sample was placed on a hot plate at about 55° C and allowed to warm. When up to temperature a few crystals of phenyl salicylate (m.p. 42° C) are placed on the sample surface. When these have melted, a transducer is placed on the liquid, and moved around to expel all the excess liquid; the sample is removed from the hot plate, and allowed to cool. Great care had to be taken with all these bonding techniques to avoid transducer breakage as the transducers are very fragile.

The sample–bond–transducer system has associated with it a transit time due to the bond, and the acoustic mismatch between the sample and the transducer. This time was evaluated graphically for RBSN samples with weight gains of approximately 22.5%, and 59%, and found to be of the order of 0.03 μsec in both cases. These samples had weight gains at the top and bottom of the available range, and the results suggested that 0.03 μsec was a reasonable correction figure to use throughout. Fig. 2 shows the graph obtained for a 59% weight gain sample.

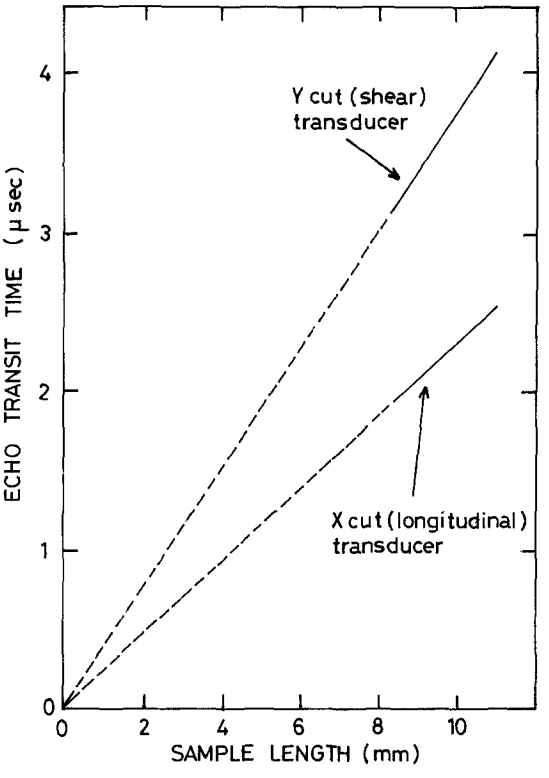

Figure 2 Transducer/bond transit time correction for a 59% weight gain RBSN sample.

3.2. Pulse echo overlap technique

The pulse echo overlap system used is shown in block diagram form in Fig. 3. The pulse modulator and receiver used was a Matec 6600 with a radio frequency (RF) plug-in module covering the frequency range 10 to 100 MHz. The unit is applicable to both single and double ended experiments, and here it was configured for single ended operation. Fig. 4 shows the single ended operation in terms of the transducer configuration, and the echoes received from the transducer. The receiver in the Matec 6600 both amplified and rectified the echoes, producing a series of echo envelopes. This meant that overlap had to be achieved using the oscilloscope Y amplifier alone. The 6600 allowed individual adjustment of pulse width, amplitude and RF frequency so that fine tuning could be carried out to obtain the most useful signal on the oscilloscope.

The whole system was triggered by a Bradley

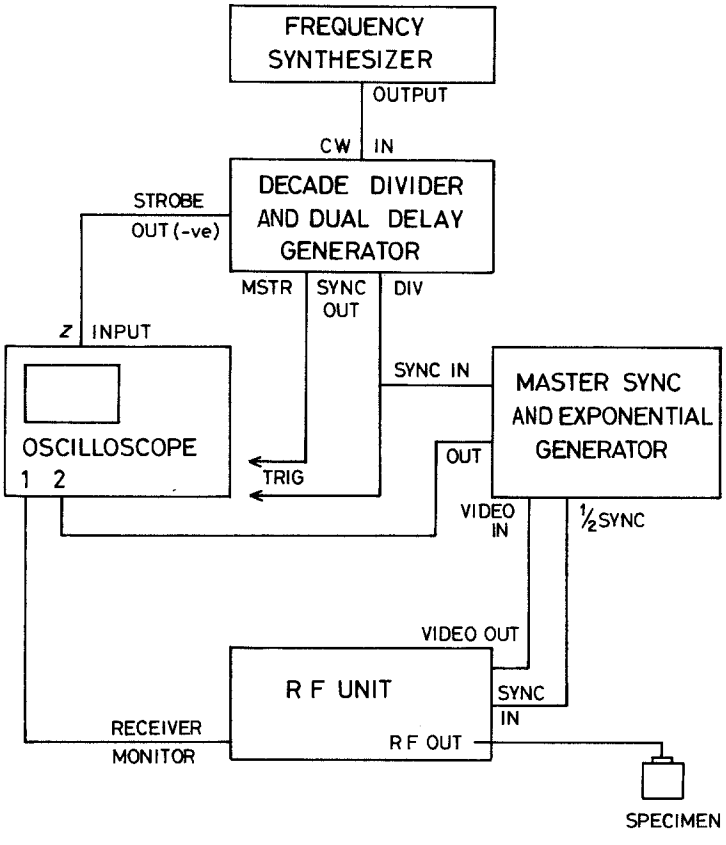

Figure 3 Block diagram of the pulse echo overlap system.

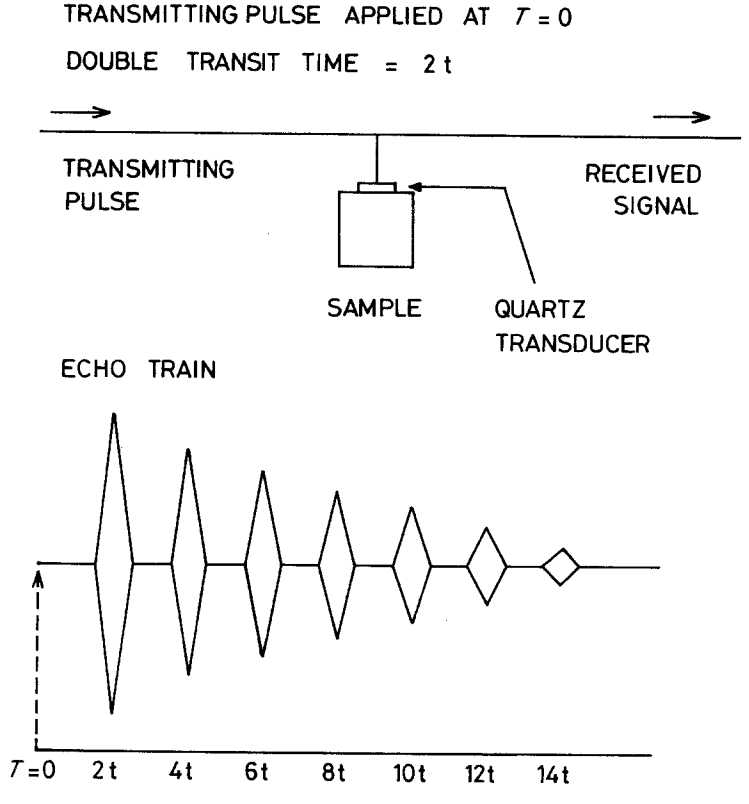

Figure 4 Single ended pulse echo method.

235 frequency synthesizer (with a stability of 1 part in 10^6) whose output was fed to the decade divider and dual delay generator. This generated synchronizing pulses at the synthesizer CW frequency, and also at this frequency divided by 10, 100, or 1000, these latter going to the master synchronizer and exponential generator (a Matec 1204A). The decade divider also provided the electronic gating necessary to observe just two overlapped echoes on the oscilloscope. The gating signal was fed to the Z input of the oscilloscope. The master synchronizer generated, on alternate synchronizing pulses, a trigger pulse for the RF generator, and an exponential. It also received the rectified echo train and made this, and the exponential available to the oscilloscope. These could be displayed separately, successively or superimposed by choice of suitable trigger input and timebase.

3.3. Experimental procedure

Initially the frequency synthesizer, set arbitrarily, was used to trigger the oscilloscope via the decade divider and the basic echo train (either RF or video) was displayed. A rough measurement of the transit time in the sample was made using the oscilloscope timebase. This was done to facilitate reasonably accurate setting of the synthesizer near to the expected result. Overlap may occur at multiples or submultiples of the correct frequency, and it was necessary to recognise and, at times avoid these frequencies, although they can be used intentionally.

The two echoes to be overlapped were chosen, and then intensified using the delay, strobe width and strobe amplifier controls of the decade divider. The rest of the echo train was suppressed on the oscilloscope by use of the oscilloscope Y amplifier, and by changing from divided to CW trigger for the oscilloscope combined with a digit by digit adjustment of the frequency synthesizer, exact overlap was obtained. In this condition the ultrasonic velocity for the RF pulse in the sample was given by

$$V_{us} = \frac{2l}{T_t} \tag{4}$$

where l is the sample length and T_t the transit time. This initial transit time was then confirmed by overlap of different pairs of echoes, both adjacent, and non-adjacent.

4. Derivation of elastic moduli

Using the pulse echo overlap technique outlined above the longitudinal and shear velocities have been measured for RBSN samples with weight gains varying from 22% to 64.5% and with densities from 1950 $kg\,m^{-3}$ to 2540 $kg\,m^{-3}$. Assuming that the materials are linear elastic (Hookeian) solids these velocities can be related directly to the elastic contents of material. The elastic constants form a fourth rank tensor, and in principle there are eighty-one of them. However, as the crystal symmetry increases the number of non-zero elastic constants decreases until for a cubic crystal, for example, there are only three independent elastic constants C_{11}, C_{12}, and C_{44}. A polycrystalline solid however can in many instances be considered to be elastically isotropic or nearly so. This is because the individual anisotropies of the randomly oriented crystallites cancel out, and an average value of elastic constants is obtained. (Exceptions to this might arise if, for example, the material were fibrous or had a preferred orientation of crystallites; as far as is known neither consideration applies to RBSN). There are thus only two independent elastic constants, namely C_{11}, and C_{12} since $2C_{44} = C_{11} - C_{12}$ for an elastically isotropic solid. In practice results are often expressed in terms of some other elastic constants (for convenience and ease of comparison), the more common being Young's modulus E, the bulk modulus K, the shear modulus μ, Poisson's ratio γ, and Lame's constants λ and μ_L. In terms of C_{11} and C_{44} the longitudinal and shear ultrasonic velocities (V_L and V_s respectively) are given by

$$V_L = \left(\frac{C_{11}}{\rho}\right)^{\frac{1}{2}} \tag{5}$$

and

$$V_s = \left(\frac{C_{44}}{\rho}\right)^{\frac{1}{2}} \tag{6}$$

(where ρ is the density of the material), and these velocities are in turn related to the elastic constants E, K and γ by the following three relationships

(a) Young's modulus, E

$$E = \frac{\mu_L(3\lambda + 2\mu_L)}{(\lambda + \mu_L)} = \frac{\rho V_s^2(3V_L^2 - 4V_s^2)}{V_L^2 - V_s^2}$$

(b) the bulk modulus, K

$$K = \lambda + 2/3\mu_L = \frac{(3V_L^2 - 4V_s^2)}{3} \tag{8}$$

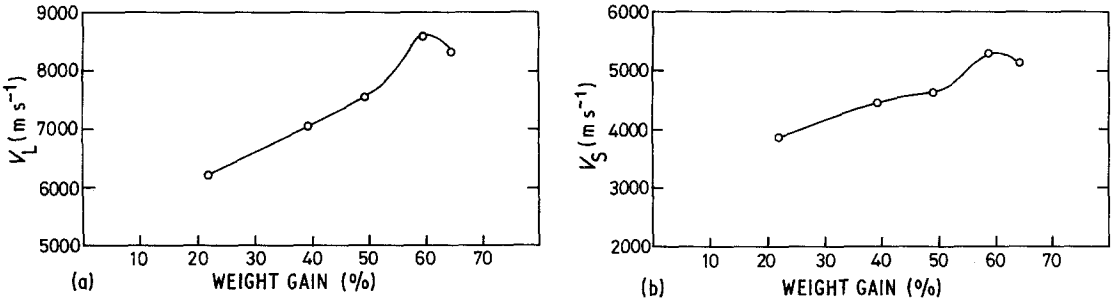

Figure 5 Variation of ultrasonic velocity with degree of nitriding, (a) longitudinal velocity V_L, (b) shear velocity V_s.

(c) Poisson's ratio,

$$\gamma = \frac{\lambda}{2(\lambda + \mu_L)} = \frac{(V_L^2 - 2V_s^2)}{2(V_L^2 - V_s^2)} \quad (9)$$

5. Results

Both the longitudinal and shear ultrasonic velocities were found to depend on the degree of nitriding which had been given to the sample during preparation. In the first instance the percentage weight gain was taken as a measure of the degree of nitriding and Fig. 5 shows the results obtained. The general trend of the variations of both longitudinal and shear velocities is to increase as the percentage weight gain increases. The effect is quite marked, the change in V_L for example being from about 6000 m sec^{-1} for 20% weight gain to around 8000 m sec^{-1} for fully nitrided material, (63% weight gain). However, closer examination of the data, particularly in the high weight gain region reveals an apparent discrepancy in the results, in that the highest velocities were recorded for 59% weight gain material. This suggested that a better approach would be to analyse the data in terms of density, or porosity. This approach reveals a rather different situation and indicates that the important factor in determining strength is not the weight gain in itself but the porosity and density of the nitride. This in turn must be related to the density of the green compact, so that a denser compact will produce a stronger product for a given weight gain.

Figs. 6 and 7 show the variations of ultrasonic velocity expressed in these terms. In Fig. 8 the longitudinal and shear ultrasonic velocities are plotted as functions of density; the graphs now show a steady rise in velocity as full nitridation is achieved. The corresponding converse effect is illustrated by Fig. 8 which shows that samples with the highest porosity give the lowest ultrasonic velocities. Here the fractional porosity, P, is given by

$$P = 1 - 0.281\,\rho_{\text{green}} - 0.148\,\rho_{\text{Nitride}} \quad (10)$$

where ρ_{green} is the density of the green compact and ρ_{Nitride} is the density of the nitride.

6. Discussion

The variations of the elastic moduli, derived from the longitudinal and shear ultrasonic velocities showed similar trends. The plots of Young's modulus (a measure of the resistance to extension) and the bulk modulus (the resistance to hydrostatic pressure) are given in Fig. 8a and b, respectively. These bear out the conclusion that the porosity

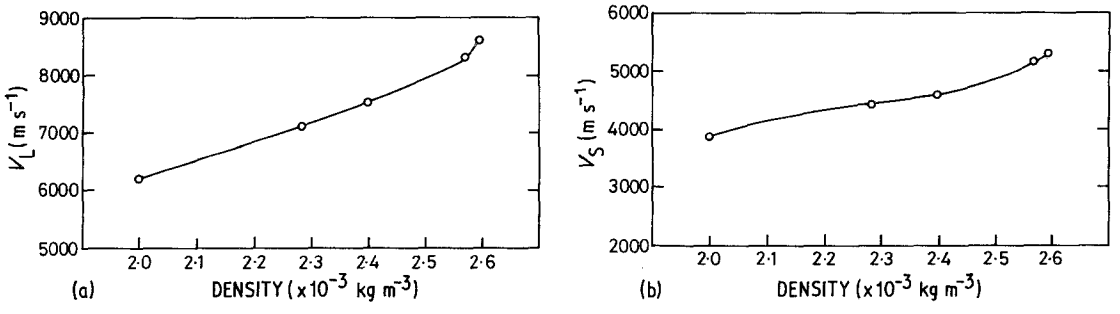

Figure 6 Variation of ultrasonic velocity with density at various stages of nitridation, (a) longitudinal velocity V_L, (b) shear velocity V_s.

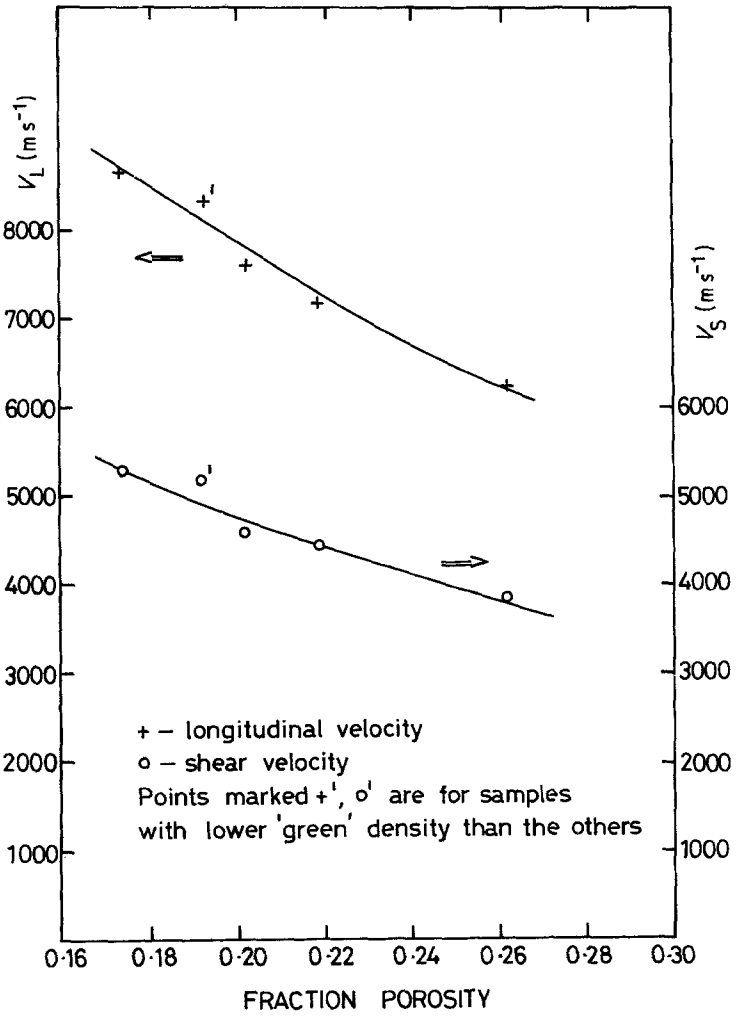

Figure 7 Porosity against ultrasonic velocity for reaction bonded silicon nitride.

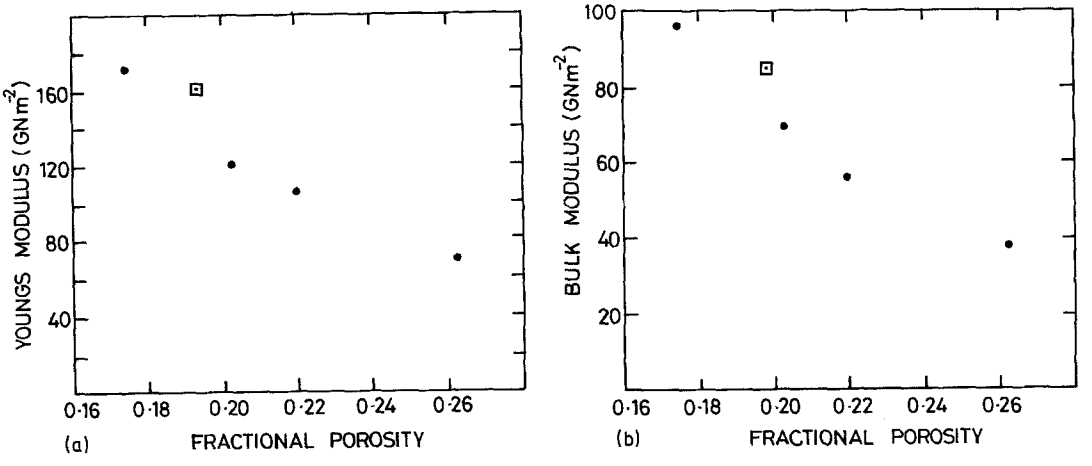

Figure 8 (a) Young's modulus against fractional porosity (b) bulk modulus against fraction porosity ○ $\rho_g = 1.6\,\mathrm{kg\,m^{-3}}$; ⊡ $\rho_g = 1.53\,\mathrm{kg\,m^{-3}}$.

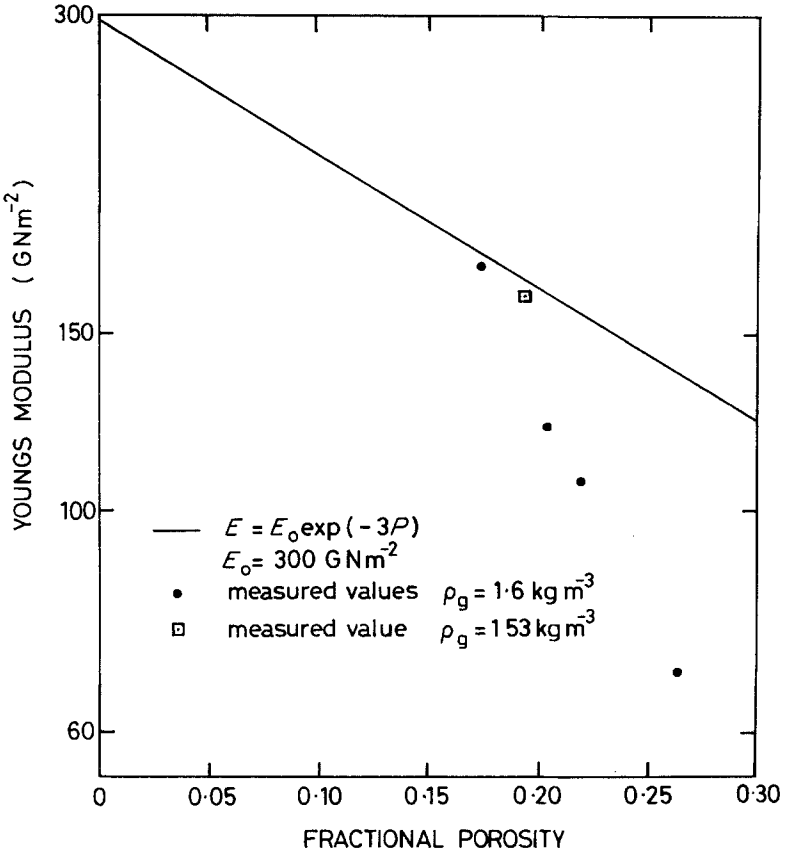

Figure 9 Young's modulus of reaction bonded silicon nitride against fractional porosity: measurement and prediction.

and density of the nitride are the main factors controlling the elastic modulus and bulk modulus.

Some further comments can be made regarding the values of Young's modulus obtained for the range of RBSN samples examined. The porosity of a ceramic can be related to the Young's modulus by the expression, [2]

$$E_p = E_0 \exp(-3P) \qquad (11)$$

where P is the fractional porosity, and E_0 the Young's modulus value for a non-porous material. E_p is the Young's modulus for a given porosity. Strictly speaking such a relation can only be applied to fully nitrided materials, i.e. to those with no unreacted silicon since E_0 must be different for a non-porous material consisting of silicon nitride and silicon. However, since this difference is likely to be small (at least for small amounts of free silicon) it is reasonable to assume that high weight gain materials would have Young's modulus close to the line $E_p = E_0 \exp(-3P)$. On this basis it would be expected that Young's modulus for low weight gain materials should fall below the same line. If a value of 300 GN m^{-2}, being the mean of several published values [11–14] of Young's modulus for hot pressed silicon nitride, is taken for E_0 in Equation 11 and the RBSN results plotted and compared with this theory (Fig. 9), this is shown to be the case.

The present work on the ultrasonic determination of the basic elastic constants of the range of partially nitrided RBSN samples, has shown that weight gain, i.e. the degree of nitridation, determines the elastic modulus of the ceramic produced. When considering two materials with similar weight gains (both nearly fully-reacted) it has been found that the material giving the larger value of elastic modulus is the one with the lower porosity and higher density, and not necessarily the higher weight gain. This indicates that the strength of an RSBN compact will depend both upon the density of the green ceramic and the weight gain as long as the weight gain is sufficiently high for the free silicon to have a negligible influence. Although an excessively dense silicon compact will inhibit the final stages of nitridation it may be advantageous in securing high strength in RBSN to use a high green density and allow some degree of incomplete nitridation.

Acknowledgements

We wish to acknowledge the help received from Advanced Materials Engineering Ltd during the course of this work.

T. G. Bushell also wishes to thank the Science and Engineering Research Council for the award of a post-graduate (CASE) studentship.

References

1. S. M. BOYER and A. J. MOULSON, *J. Mater. Sci.* **13** (1978) 1637.
2. A. J. MOULSON, *ibid.* **14** (1979) 1017.
3. J. T. MILEK, "Handbook of Electronic Materials", Vol. 3 (IFI/Plenum, New York, 1971).
4. W. M. WELLS, *Univ. Calif. Res. Lett.* **77** (1964) 95.
5. J. D. WALTON, *Amer. Ceram. Soc. Bull.* **53** (1974) 255.
6. S. N. RUDDLESDEN and P. POPPER, *Acta Crystallogr.* **11** (1958) 465.
7. T. G. BUSHELL, PhD thesis, University of Durham (1983).
8. H. J. MCSKIMIN and P. ANDREATEH, *J. Acoust. Soc. Amer.* **34** (1962) 609.
9. H. J. MCSKIMIN, *ibid.* **22** (1950) 413.
10. N. G. PACE, PhD thesis, University of Durham (1970).
11. R. W. JONES, K. C. PITMAN and M. W. LINDLEY, *J. Mater. Sci.* **12** (1977) 563.
12. W. A. FATE, *J. Appl. Phys.* **46** (1975) 2375.
13. A. GIACHELLO, P. C. MARTINENGO, G. TOMASINI and P. POPPER, *Amer. Ceram. Soc. Bull.* **59** (1980) 1212.
14. O. YEHESKEL, Y. GEFEN and M. TALIANKER, *J. Mater. Sci.* **19** (1984) 745.

Received 26 June
and accepted 7 September 1984